

Performance Optimisation of an Extended Dynamic Range Microwave Photonic Link with Dual Link Architecture

Manik Attygalle, Tim Priest, Kamal Gupta and David Hunter
Electro Optic Group, EWRD
Defence Science & Technology Organisation, Edinburgh, SA, 5111, Australia
Email: manik.attygalle@dsto.defence.gov.au

Abstract: The paper presents the performance optimisation, through RF-photonic simulation, of a microwave photonic link that is suitable for EW applications that exhibits an increased dynamic range compared to conventional microwave photonic links. It utilises a dual optical link architecture to realise the extended dynamic range (> 100 dB). The simulations take into account the RF pre- and post-amplification differences and detailed parameters of the lasers, RF amplifiers, optical intensity modulators and photo-detectors used in the system.

1. Introduction

Micro/Milli-metre wave photonic links (MPL) offer a number of significant advantages over coaxial cable microwave links in variety of defence applications. These include low loss (~ 0.2 dB/km) and weight, high bandwidth and immunity to EM interference. Electronic warfare (EW) systems are one such example where MPLs can be used to connect EW receivers having spatially separated antenna elements. To-date, the major barriers for the ubiquitous use of these links in these applications have been the relatively higher noise figure (NF) and limited dynamic range compared with coaxial cable links. These limitations are primarily due to the inefficient electric-to-optic-to-electric conversion and additional noise added by the active photonic components.

Past techniques to increase the dynamic range of MPLs have focussed on lowering the noise in the link, increasing optical linearity of the modulator, increasing optical power at the photo-detector (PD), or optical carrier suppression to reduce optical power saturation at the PD [1-5]. However, these methods have a number of limitations that restrict the sensitivity and/or the bandwidth over which they are useful. The Electro-Optic Technologies (EOT) group in DSTO have developed a novel extended dynamic range MPL (EDR-MPL) architecture to enhance both the compressive and spurious-free dynamic range in comparison to a conventional MPL [6]. The technique utilises switching logic using a *PIN* diode switch for selective switching between two MPLs running in parallel to realise the higher dynamic range in comparison to the conventional MPL. The architecture utilises a photonic feed-forward gain control mechanism that overcomes some of the problems associated with automatic gain control.

2. Micro/MM-wave Photonic Dual Link Architecture

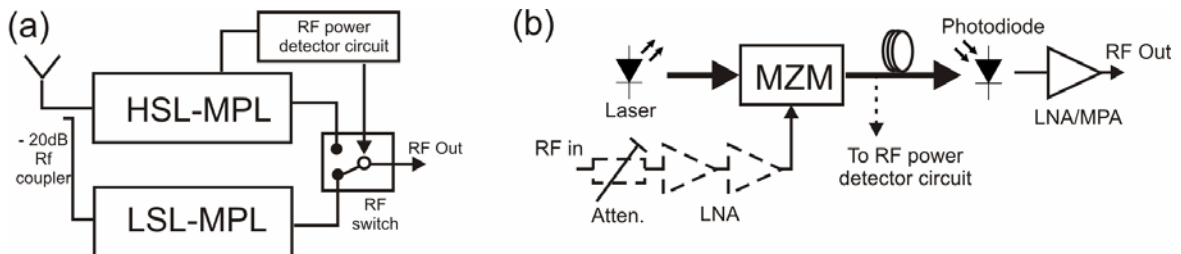


Fig. 1: (a) Schematic showing the EDR-MPL with dual link architecture and (b) Simulation model used to analyse both the HSL and LSL.

Fig.1 (a) shows the architecture of the EDR-MPL system consisting of two photonic links: one a high sensitivity link (HSL) and the other a low sensitivity link (LSL), which constitutes two

different signal paths. The output from the EDR-MPL can be input into either an analogue or digital receiver for EW processing. In the HSL, the majority of the incoming RF signal power (typically 99%) obtained through an RF directional coupler is amplified by high gain, low noise amplifiers (LNA) and modulated onto an optical carrier using an external optical modulator such as a Mach-Zehnder Modulator (MZM) and transmitted over a fibre link. This link is designed to transmit very low power incoming RF signals, thereby increasing the sensitivity of the overall link. However, for stronger input power levels, this link undergoes saturation and/or distortion due to the nonlinear transfer function of the MZM. On the other hand, in the LSL, the attenuated RF signal from the directional coupler (-20 dB) passes through unamplified or with a lower gain than the HSL that allows higher power RF signals to be transmitted through the optical link without distortion. This link allows larger input power levels but will be less sensitive to “weak” incoming RF signals. A switching logic circuit is used to input signals into the digital receiver depending on the detected power. Typically, a small proportion (5-10%) of the optical power from the HSL will be tapped off to enable the switching circuitry and the fibre link provides sufficient delay for the switching latency.

The aim of this work is to investigate the optimum architecture and component specifications to provide the optimum dynamic range and noise performance for the EDR-MPL. Fig. 1(b) shows the model used in the simulation for the HSL and LSL. The components indicated by the dashed line show optional modules in the simulation. The HSL can have one or two RF pre-amplifiers to give the necessary gain, while the LSL will have one or no (un-amplified) pre amplifiers or even an RF attenuator. In addition, at the output of the photo-detectors, the HSL will have a low noise post-amplifier (LNA) while the LSL will have microwave power amplifier (MPA) for post detection RF amplification so as to achieve the highest signal power.

3. Simulation

A detailed numerical simulation was carried out to optimise the performance of the EDR-MPL architecture. A range of photonic and RF parameters were investigated to ascertain their effect on the performance of the EDR-MPL, as shown in Table 1.

Variable	Range	Units
Laser relative intensity noise (RIN)	-120 to -170	dB/Hz @ 50 mW
Laser power	25 to 100	mW
Linewidth	2 to 10	MHz
MZM V_{π} (RF)	3 to 6	V
MZM insertion loss	3 to 6	dB
MZM extinction	15 to 30	dB
PD responsivity	0.5 to 0.95	A/W
PD dark current	10	nA
PD thermal noise	10×10^{-12}	A/ $\sqrt{\text{Hz}}$
RF amplifier gain	20 to 40	dB
RF amplifier NF	2.5 to 6	dB
RF amplifier saturation power	30	dBm

Table 1: Variable parameters and the value ranges used in simulation.

The simulation was carried out with 1 MHz frequency resolution. This value was selected according to the characteristics of the digital receiver to be used for processing of the received signals, which requires signals to be typically 10 dB above the noise floor (at 100 KHz bandwidth). The results presented in this paper are for a 10 GHz input signal with the RF amplifier frequency range of 2-18 GHz. However, the results can be easily extended to cover the 2-40 GHz range.

4. Results and Discussion

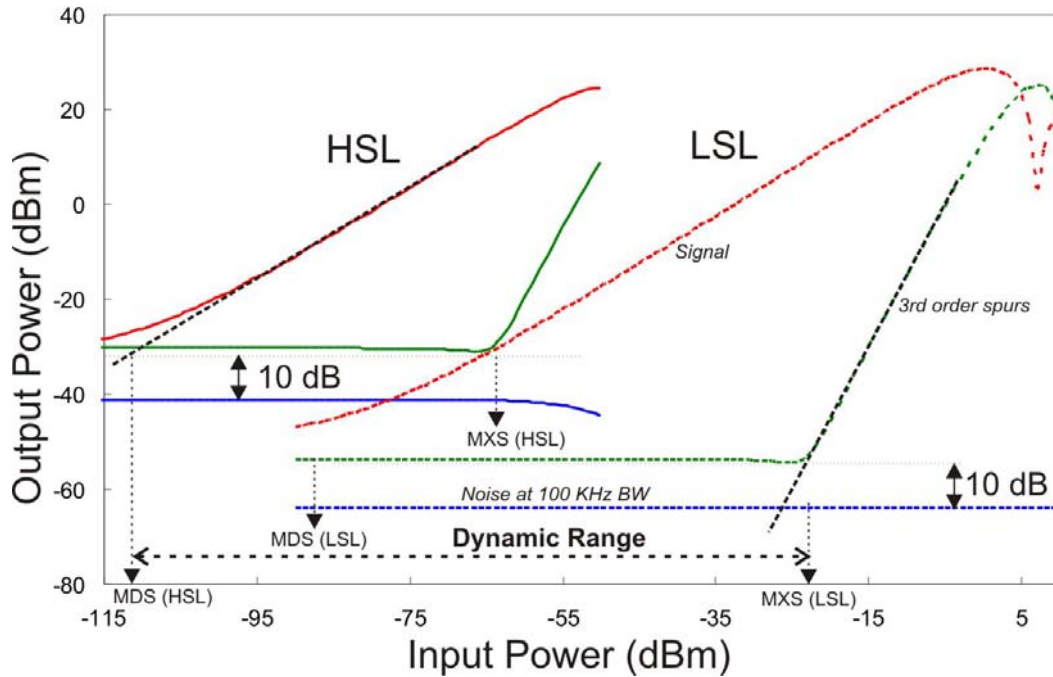


Fig. 2: Output power vs Input power for typical HSL (solid) and LSL (dashed). The figure also depicts the defined MDS and MXS parameters for both the HSL and LSL.

Fig. 2 shows the typical input output curves for the HSL (solid) and the LSL (dashed) which shows the lines for the output signal power, noise power (in 100 KHz bandwidth) and power of the 3rd order spurious products. The HSL is constrained by the minimum detected output power at low input power levels while the output will be switched to the LSL when output of the HSL starts to compress. On the other hand, the LSL will be constrained by the onset of spurious signals due to MZM nonlinearity and saturation of the RF post-amplifier at high input power.

In this work, the minimum detectable signal (MDS) is defined as the input power when the output power is 10 dB above the noise floor (in 100 KHz BW) as required by the digital receiver. Consistent with the MDS, the maximum input signal (MXS) is defined as input power when spurious signal power is 10 dB above the noise power. To optimise the performance and increase the dynamic range of the EDR-MPL the MDS should be reduced by increasing the sensitivity of the HSL. Simultaneously, the MXS of the LSL should be increased by delaying the onset of spurs while keeping an appropriate overlap between the two curves so that switching between the HSL and LSL can be performed seamlessly and without degradation, for any input power range. In other words the MXS of the HSL needs to be larger than the MDS of the LSL by approximately 10 dB. Then the total dynamic range is the input range between MDS of the HSL and MXS of the LSL. In the next subsections the HSL and LSL are analysed separately to evaluate the effects of the different variables on the link performance.

4.1. High Sensitivity Link

Fig. 3 shows the Noise Figure when (a) the MZM $V\pi$, (b) MZM insertion loss, (c) laser power and (d) laser RIN, is varied respectively, while all other parameters are kept constant (laser linewidth = 5 MHz, laser power = 75 mW, RIN = -150 dB/Hz, MZM $V\pi$ = 5 V, insertion loss = 3 V, MZM extinction = 30 dB, PD responsivity = 0.85, NF of RF amplifiers = 3 dB). The diamonds in the figure indicate the HSL with two cascaded 30 dB RF pre-amplifiers, while the squares depict when there is only one 35 dB RF pre-amplifier. Note, $V\pi$ is the half wave switching voltage of the optical modulator.

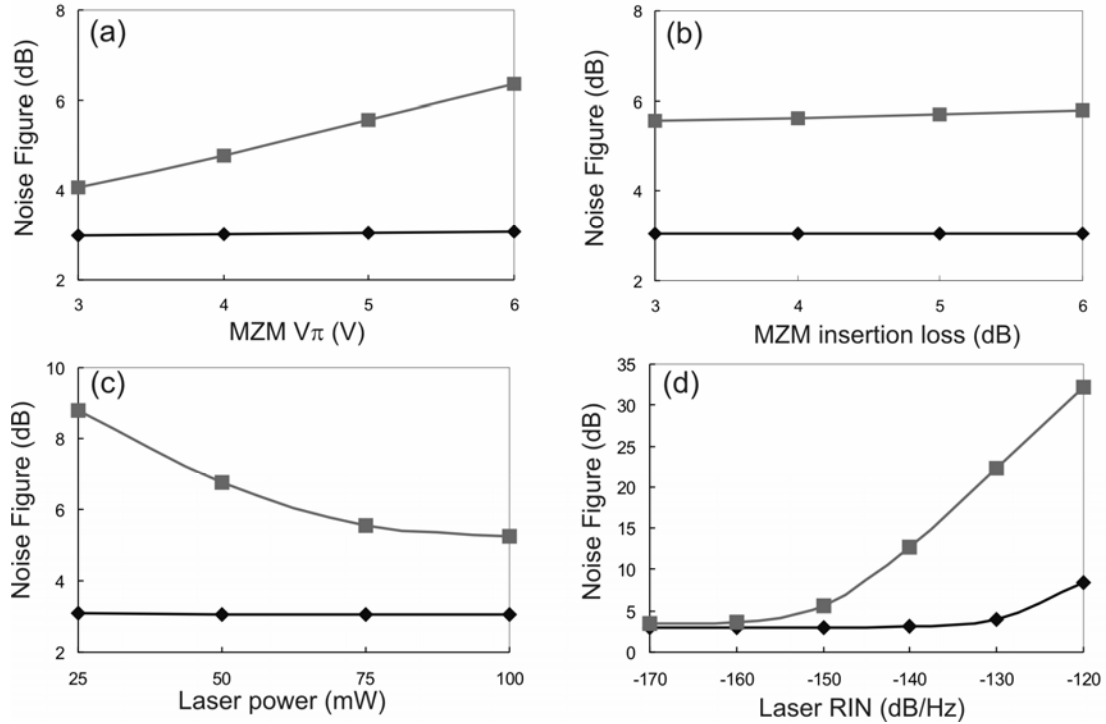


Fig. 3: Noise Figure for the HSL against (a) MZM half wave switching voltage (b) MZM insertion loss (c) Laser power and (d) Laser RIN. The diamonds represent HSL with two cascaded pre-amplifiers with 30 dB gain each and squares are for HSL with one 35 dB pre-amplifier.

The noise performance of the HSL with higher pre-gain (with the cascaded RF amplifier configuration) is governed by the noise performance of the amplifiers as expected. There is a NF penalty only when the RIN of the laser is above -140 dB/Hz. On the other hand the NF varies with the optical component variables when there is less pre-amplifier gain with the use of a single RF amplifier. In this case a smaller V_{π} and higher laser power shows best noise performance.

Fig. 4 shows the MDS for the HSL when (a) the MZM V_{π} and (b) MZM insertion loss is varied with other parameters kept constant as before. It is observed that the MDS can be maintained at -111 dBm with a higher RF pre-gain (with the cascaded RF amplifier configuration) in the HSL while the MDS is reduced to approximately -105 dBm with lower RF gain (one RF pre-amplifier). It also shows that when two amplifiers are used the stringent requirements of the optical components such low MZM V_{π} and low laser RIN can be relaxed. It is noted that the MXS of the HSL with the two RF pre-amplifiers is at -62 dBm which will give sufficient overlap between the LSL dynamic range to provide automated switching.

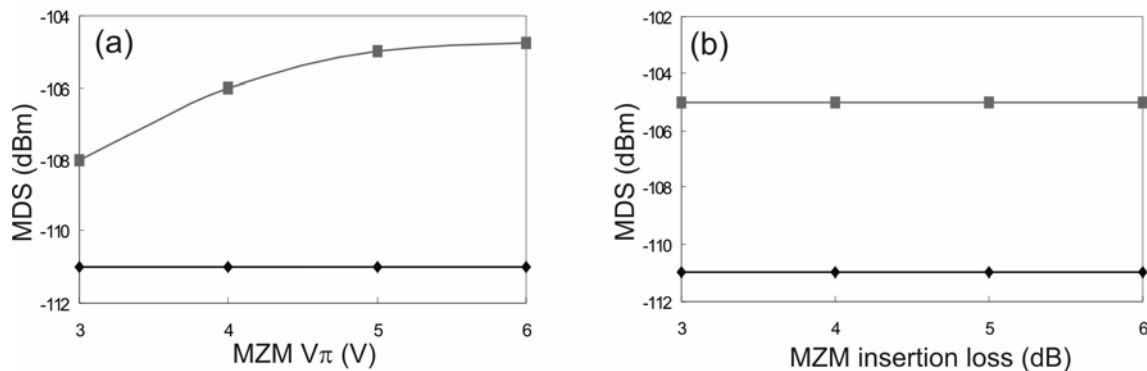


Fig. 4: MDS for the HSL against (a) MZM half wave switching voltage and (b) MZM insertion loss. The diamonds represent HSL with two cascaded pre-amplifiers with 30 dB gain each and squares are for HSL with one 35 dB pre-amplifier.

4.2. Low Sensitivity Link

Fig. 5 shows the Noise Figure for the LSL when (a) MZM $V\pi$, (b) MZM insertion loss, (c) laser power and (d) laser RIN is varied with other parameters kept constant. The diamonds are for a LSL with one 30 dB RF pre-amplifier and the squares depict when there is an additional 10 dB attenuator before the pre-amplifier. The circles represent when there is no RF pre-amplifier or attenuator and when a -10 dB RF coupler is used instead of the -20 dB RF coupler at the input.

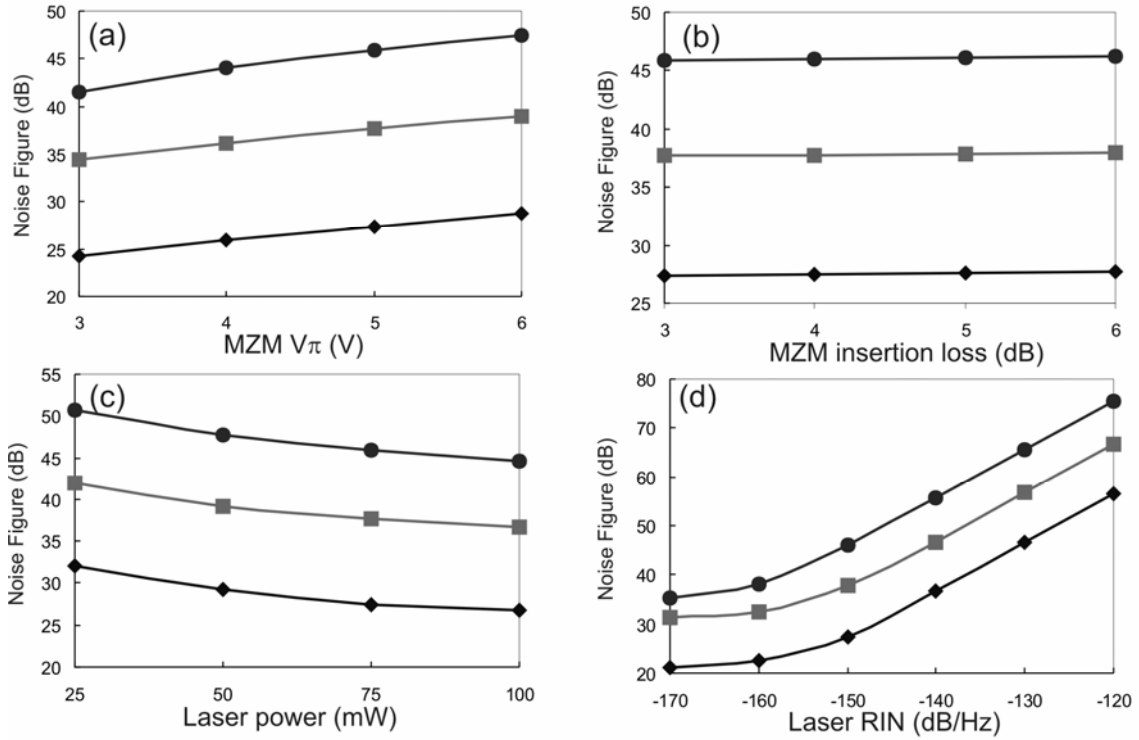


Fig. 5: Noise Figure for the LSL against (a) MZM half wave switching voltage (b) MZM insertion loss (c) laser power and (d) laser RIN. The diamonds represent LSL with a pre-amplifier with 30 dB gain and squares with an additional 10 dB attenuator. Circles are with a -10 dB RF coupler without any amplifier or attenuator.

The NF of the LSL is significantly larger than the HSL and the effects of the laser power and RIN are more pronounced. However, it should be noted that the function of the LSL is to increase the MXS whilst keeping reasonable noise performance. Fig. 6 shows the MXS for the LSL when (a) the MZM $V\pi$ and (b) MZM insertion loss is varied with other parameters kept constant. The MXS is approximately -20 dBm with no attenuator, and -10 dBm when a 10 dB attenuator is used before the pre-amplifier. As expected, the MXS is larger by 10 dB when a 10 dB attenuator is used. However, it should be noted that the MDS of this link would increase when larger attenuators are used and there will be no overlap between the HSL and LSL to facilitate switching without degrading the performance. The MDS for the LSL with the 10 dB attenuator was measured to be -72 dBm while the MXS for the HSL with two pre-amplifiers was -62 dBm which gives the required 10 dB input range overlap between the two links. The MXS of the HSL without any amplifiers was only -63 dBm and therefore ignored in the rest of the analysis. Further, we also note that larger $V\pi$ will give larger MXS with the other parameters kept constant, while the insertion loss of the MZM does not have a significant effect on the MXS of the link. As a result, a MZM with larger $V\pi$ will be preferable for the LSL.

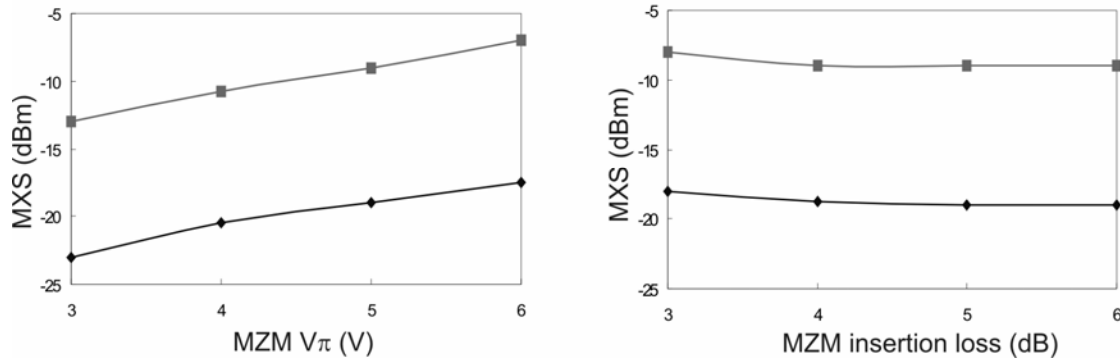


Fig. 6: MXS for the LSL against (a) MZM half wave switching voltage and (b) MZM insertion loss. The diamonds represent LSL with a pre-amplifier and squares represent LSL with an additional 10 dB attenuator.

5. Conclusion

The paper presented detailed simulation study of an extended dynamic range MPL with dual link architecture. It consists of a high sensitivity link with the function of reducing the minimum detectable signal power (MDS) and a low sensitivity link with the aim of increasing the maximum input power (MXS) while keeping input power overlap such that the switching logic can switch between the two links when input signal power changes. The noise and dynamic range of the links were evaluated with different component variables within practical limits to obtain the best performance for the links. The optimum EDR-MPL was observed to be a HSL with two cascaded pre-amplifiers (to give the necessary RF gain) with a lower MZM switching voltage; and a LSL link with a 10 dB attenuator and one RF pre-amplifier and a MZM with a higher switching voltage. A total dynamic range of more than 100 dB can be achieved with the MDS below -110 dBm and the MXS above -10 dBm using this EDR-MPL configuration.

Acknowledgment: The authors would like to thank Richard Lindop, Tony Lindsay, Linh Nguyen, Geoff Knight, Mike Parker and Leigh Milner for helpful discussions.

6. References

- [1] M. L. Farwell, W. S. C. Chang, and D.R. Huber, "Increased linear dynamic range by low biasing the Mach-Zehnder modulator", IEEE Photon. Technol. Lett., vol. 5, no. 7, pp. 779-782, July 1993.
- [2] M. J. LaGasse, W. Charczenko, M. C. Hamilton, and S. Thaniyavarn, "Optical carrier filtering for high dynamic range fibre optic links", Electron. Lett., vol. 30, pp. 2157-2158, Dec. 1994.
- [3] R. D. Esman, and K. J. Williams, "Wideband efficiency improvement of fibre optic systems by carrier subtraction", IEEE Photon. Technol. Lett., vol. 7, pp. 218-220, Feb. 1995.
- [4] T.E. Darcie and P. F. Driessen, "Class-AB Techniques for high dynamic range microwave photonic Links" IEEE Photon. Technol. Lett., vol. 18, pp. 929-931, Apr. 2006.
- [5] A. Karim and J. Devonport, "Noise Figure reduction in externally modulated analog fiber-optic links" IEEE Photon. Technol. Lett., vol. 19, pp. 312-314, Mar. 2007.
- [6] K. K. Gupta, T. S. Priest and D. A. Palumbo, "Design of a Microwave Photonic Link with Extended Dynamic Range for Advanced Electronic Warfare Systems" DSTO-RR-0307, Feb. 2006.